J. Membrane Biol. 56, 183–190 (1980)

The Journal of
Membrane Biology

Flow through Brushborders and Similar Protuberant Wall Structures

D. Basmadjian, D.S. Dykes, and A.D. Baines

Department of Chemical Engineering and Applied Chemistry and Department of Clinical Biochemistry, University of Toronto, Toronto, Ontario, M5S 1A4

Summary. Longitudinal flow through channels with protuberant wall structures such as brushborders were studied both experimentally and theoretically. The experiments were performed using tubes with synthetic internal brushborders, scaled to resemble the geometry and flow in proximal tubules of the kidney. Fractional flow rates in the brushborder were deduced from transit times of dye traces through the central core and total flow rate. The measured ratios of brushborder to core flow Q_B/Q_C were found to be independent of Reynolds number over the range $Re = 0.01 - 0.2$. They agreed reasonably well with theoretical predictions based on the Kozeny-Carman equation for flow through arrays of parallel cylinders. The predictions can be extended to arbitrary geometries and turbulent flow conditions by appropriate modifications. Extrapolation of the results to the proximal tubule of the kidney indicate that brushborder flowrates there vary from 0.003 to 0.09% of total flow. Any axial transport in these structures would be predominantly diffusive in nature, and would be highly unlikely to affect radial brushborder gradients and transmural flux.

Structures containing brushborders made up of microvilli or other wall protuberances occur in a variety of animal and human organs, including the proximal convoluted tubule of the kidney, and the intestine. When exposed to a flowing fluid, part of that fluid passes through the voids of the protuberant structure in a direction parallel to the main flow. The magnitude of this interstitial flow depends on the available free cross sectional area as well as the resistance offered by the protuberant structure.

In renal proximal tubules, the brushborder appears very dense, but measurements on rabbit [10] and rat [9] tubules indicate that the space between microvilli is at least equal to 40% of the central luminal core. Thus a considerable proportion of total axial flow down the tubule could pass through the brushborder. Obviously the numerous microvilli will impede fluid flow, but the magnitude of the resistance cannot be measured *in vivo*. If the resistance is low enough to allow a substantial interstitial flow to develop, radial gradients in the brushborder could be significantly altered. More importantly, the effect on the gradients would be sensitive to changes in axial flow. Two major recent reviews of proximal tubular function [3, 4] contain speculation that changes in unstirred layers within the brushborder may indeed by responsible for flow dependent absorption in the proximal tubule. In a relevant theoretical study, Richardson, Licko and Bartoli [8] have shown that "stirring" of fluid in the brushborder could significantly alter transport into the cell.

At present there are no experimental data available to confirm these hypotheses or to provide a general basis for predicting flow rates in brushborders and similar wall structures. A knowledge of these flow rates is a prerequisite for assessing the effect of axial convective flow on radial (transmural) transport.

In an effort to provide this information, we initiated a study of flow through channels with protuberant wall structures such as those found in renal tubules and the intestine. For our experiments we constructed a series of tubes with artificial internal brushborders resembling those observed in the proximal tubule. Fractional flow rates were measured over the physiologically important range of Reynolds numbers $0.01 - 0.2$. In these first experiments, no attempt was made to study the effect of pulsatile flow, microvilli motions, or leakage through the tubule wall, since this would have unduly complicated an already delicate measuring technique. As is shown later, these factors are unlikely to alter significantly

0022-2631/80/0056-0183 $01.60

the results and conclusions of this work. The theoretical correlations we obtained appear to be general enough to allow extrapolation to other geometries and flow regimes as well.

Materials and Methods

1. Construction of Brushborder Tubes

An initial difficulty was the construction itself of the brushborder tubes. One unit of 10 cm length was prepared by drilling closely spaced holes into a Lucite tube of about 3.25 cm diameter. Tufts of some 12 bristles held together by a copper clip were mounted and glued into the openings. This is the conventional manner of constructing commercial brushes but does not give the desired individual spacing of bristles which more closely corresponds to the structure of physiological brushborders. The unit was nevertheless used to supplement our experiments with other structures.

A search of commercially available materials led to the choice of a device used in cleaning copper pipe and battery terminals. In these units, the internal "brushborder" consists of metal staples which are punched into a cylindrical plastic mantle. The individual bristles are spaced approximately 1 mm apart and can be thinned out by selective removal of staples. We chose a type having stainless steel staples because of the slightly corrosive medium used. Eight of the units, each about 1.25 cm long, were glued together with epoxy resin for an overall length of 10 cm and sealed into a Lucite tube of about 3.2 cm ID. Two sparser versions were obtained by removing one-half and three-quarters of the staples, respectively. Photographs of an individual unit and the assembled brushborder tube are shown in Fig. 1.

The tubes constructed in this fashion yielded brushborders with void fractions ε of 0.93–0.99 at the bristle base, converging to values of 0.79–0.98 at the tips. A further extensive search of commercial sources turned up only one denser material, Brushlon (3M International Operations, St. Paul, Minn.), consisting of an array of individual nylon bristles mounted on a flat polyurethane backing. In spite of the seemingly high base void fraction ($\varepsilon = 0.88$), the bristle packing was in fact quite dense and considerable difficulty was experienced in rolling the material into tubular shapes. The final void volume at the bristle tips was 0.678. It is doubtful that this density can be easily exceeded in other artificial brushborder constructions.

A summary of all pertinent dimensions of the tubes used in this work appears in Table 1.

2. Flow Rate Measurements

Initial experiments consisted of collecting fluid separately from the brushborder and core of the tube. This led to spurious values due to small differences in the pressure drops through the collector tubes. The results were consequently discarded. We next attempted to introduce a well-defined dye trace upstream of the brushborder to allow us to measure transit times. The procedure proved to be unreliable due to the erratic and unpredictable course of the trace. The anomaly was attributed to diffusional and density effects which emerge as significant factors at the low flow rates in question.

To overcome this difficulty, we used an ingenious method developed by Baker [1] in which an acid-base indicator titrated to the end point is dissolved in the fluid. A potential applied to electrode grids placed directly in the flowing medium results in a local pH change causing the indicator to change color. The dye

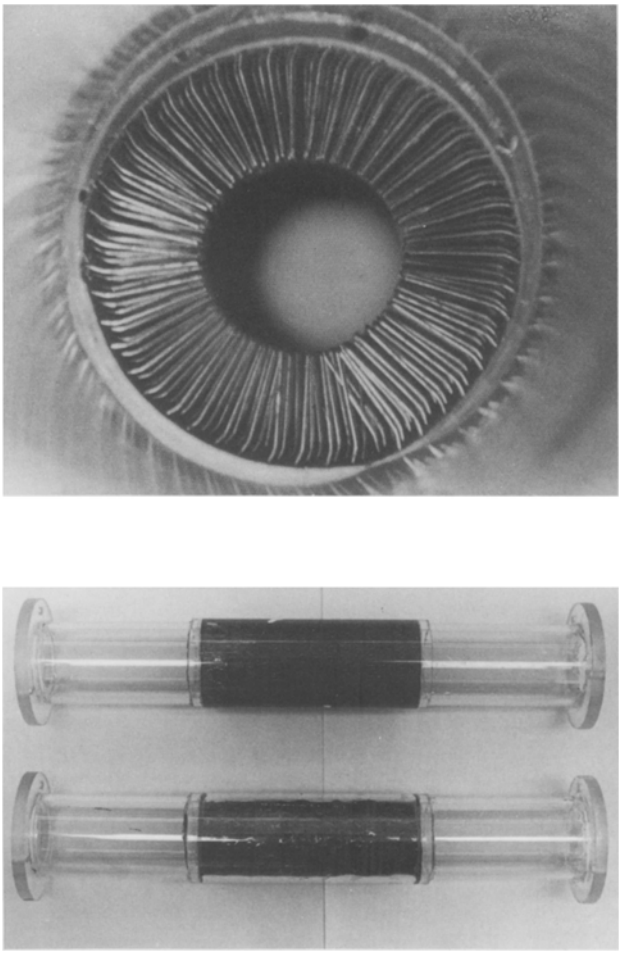

Fig. 1. Construction of a wire brushborder tube

streaks produced in this fashion are carried along individual streamlines without being subjected to the distorting forces mentioned previously. Only the core flow rates (Q_C) were measured by this method. The flow rate through the brushborder, Q_B, could not be determined directly because of the inevitable dispersion of the trace and was calculated by subtracting core flow from total flowrate, Q_T. A more direct confirmation of the presence of flow was obtained by photographs of the traces during their approach to the brushborder (Fig. 2).

In a first set of experiments, a tube of precisely known dimensions was fitted tightly into the core of the brushborder tubes. This ensured uniform channel geometry and avoided distortion of the trace by "slip" (i.e., nonzero velocity) at the brushborder interface. The tube was allowed to protrude slightly at both ends of the brushborder to allow precise visual observation of the entry and emergence of the dye trace. The results were thus well-suited for a preliminary validation of the hydrodynamic relations given in our theoretical development. Brushborder-to-core flow rates obtained in these experiments were subsequently translated into flow ratios which would prevail in the absence of tubular inserts by means of appropriate corrections.

In a second and independent set of experiments, the measurements were duplicated without the use of tubular inserts. These results were somewhat less reliable because of unavoidable slight variations in core dimensions and difficulties in observing the exact time of dye entry and exit. Since core flow rates constituted the

Table 1. Details of Brushborder Tubes

Type	Brush length (cm)	Core diameter (cm)	Bristle material	Bristles			Brush void volume		
				Length (cm)	Diameter (cm)	No. per cm^2	At wall	At core	Average
Pipe cleaners									
High density	10.60	1.491		0.870	0.0333	42.1	0.9632	0.9204	0.9496
Medium density	10.51	1.488	Stainless steel	0.870	0.0333	21.1	0.9816	0.9605	0.975
Low density	10.57	1.487		0.870	0.0333	10.5	0.9908	0.9803	0.9873
Brushlon	8.85	0.997	Nylon	0.825	0.0256	227	0.8835	0.6779	0.839
Own construction	10.00	1.119	Nylon	1.078	0.0203	224	0.9274	0.7874	0.892

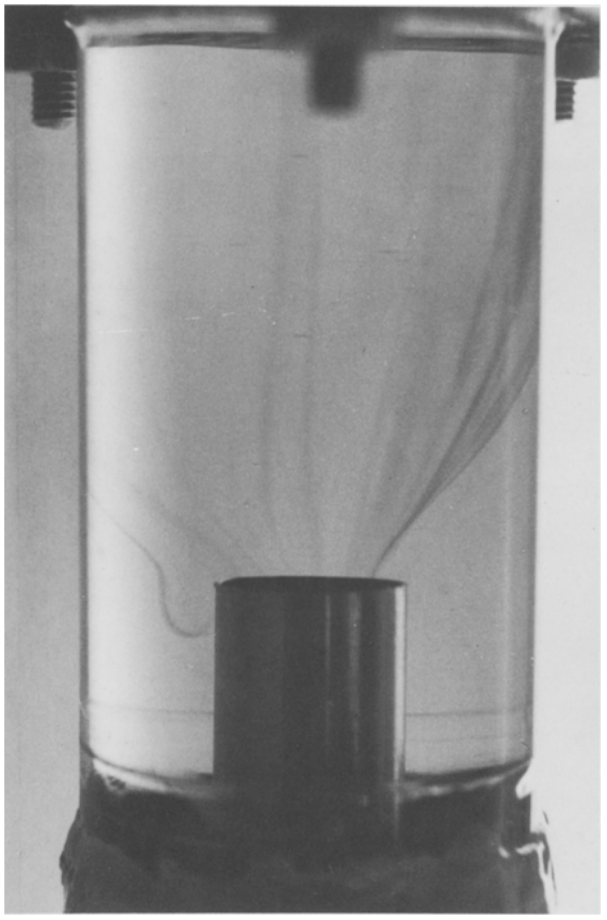

Fig. 2. Photograph of dye trace near the entrance to the brushborder tube

major fraction of total flow, small changes in these parameters had a significant effect on computed values of brushborder flow. Estimates of these errors were included in the interpretation of the experimental results.

In order to assess the error associated with the dye-trace technique itself, dummy runs using a smooth-walled cylindrical tube were conducted over the same range of Reynolds number. The difference between the measured values of Q_C and flow rates calculated from the weighed effluent agreed within $\pm 2\%$ over most of the range, the error rising to slightly below $\pm 3\%$ at the lowest Reynolds numbers. Tube diameters were measured to ± 0.2 mm, transit times within an estimated $\pm 2\%$.

3. Experimental Apparatus and Procedure

A schematic diagram of the experimental apparatus is shown in Fig. 3. The test fluid containing the dye was supplied from a constant-head reservoir and flowed through a rotameter to the horizontally mounted tubular section. Tapered Lucite pipes were provided both upstream and downstream from the test section to eliminate abrupt changes in flow pattern. The electrodes used to generate the dye trace consisted of two grids made of 0.64 mm diameter platinum wire, both 2.5 cm square and spaced approximately 3 mm apart. Voltage supply came from a Heathkit model PS-3 variable DC unit (Heath Company, Benton Harbour, Mich.).

The test fluid was prepared by thoroughly dispersing chlorophenol red indicator (1% solution in 20% ethanol) in an aqueous solution of approximately 85% glycerol. About 20 ml of indicator solution was used per liter solution. The pH was then carefully adjusted by dropwise addition of 0.1 N HCl until the solution just turned yellow (pH of about 4.6). Viscosities and densities of representative samples were determined at 20 and 25 °C using an Ostwald viscometer and Westphal balance ($\mu = 98.8$ cP, $\rho = 1.2256$ g/cc at 20 °C).

Prior to commencing a run, the assembly was mounted vertically and allowed to fill with test solution to displace the air. It was then returned to a horizontal position. The flow was started and kept at a precisely constant value by fine adjustment of the rotameter control valve. Effluent was collected through a 1-mm capillary tube and weighed at appropriate intervals to ± 0.01 g.

Upon activating the power supply, a slow emergence of red dye streaks from the electrodes was observed which gradually developed into a three-dimensional network of parabolic traces. After about 2 min, the power was turned off. Recording of the transit time was commenced when the *tip* of the leading trace entered the free core and terminated upon its emergence at the center of the downstream end. The time of passage ranged from approximately 10 to 700 sec, core flow rates from about 0.01 to 0.25 cc/sec over the Reynolds number range investigated.

Results

1. Experiments with Tubular Inserts

The tubular core flow rate Q^1, can be obtained from measured transit times t of the trace tip via the relation

$$Q_C^1 = \tfrac{1}{2}(V_C/t) \qquad (1)$$

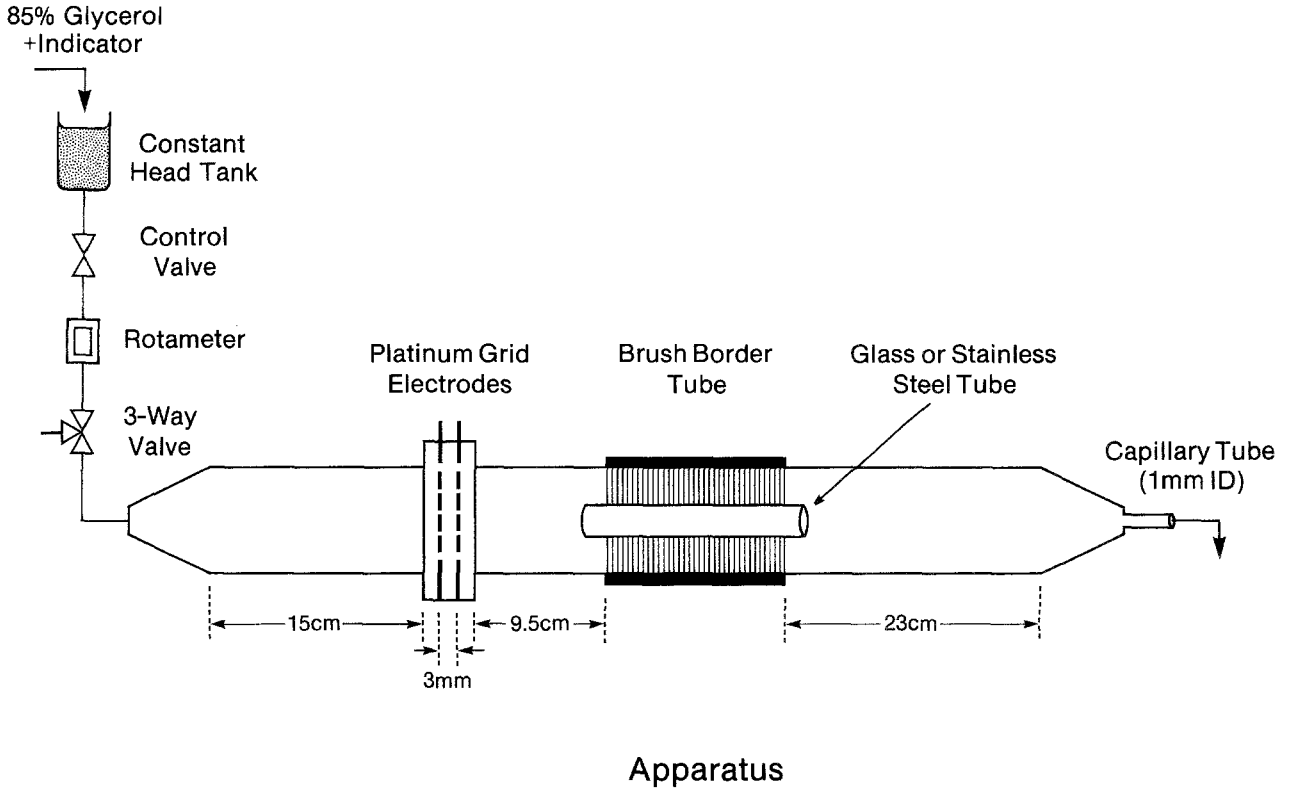

Fig. 3. Schematic diagram of experimental apparatus with tubular insert

where V_C = free volume of the tubular insert. The expression assumes viscous flow with no slip at the wall of the insert. The brushborder flow in the presence of inserts, Q_B^1, is obtained by subtracting Q_C^1 from total flow rate Q_T^1.

To translate these measurements into flow ratios Q_B/Q_C which would prevail *in the absence of inserts*, corrections have to be applied to account for tube wall thickness and for slip at the brushborder interface. This is not the simple matter it appears to be since both flow rate and pressure drop change when the insert is removed. We note, however, that the ratio of the two quantities remains constant provided there is no change in flow regime associated with tube removal. This was confirmed by the linear relation obtained when Q_B^1 is plotted against $\Delta P/\mu$ calculated from Poiseuille's law and measured tubular core flow. The slope of this plot, $m = Q_B^1 \mu/\Delta P$ is used to convert Q_B^1/Q_C^1 obtained with tubular inserts into flow ratios Q_B/Q_C for brushborders without inserts.

To implement this conversion, we first derived the flow rate/pressure drop relation for laminar flow with slip at the tube wall. If slip velocity is assumed equal to the average velocity in the brushborder, one obtains:

$$Q_C = \frac{\pi D_i^4 \Delta P}{128 \mu L} + Q_B \frac{D_i^2}{D_o^2 - D_i^2} \tag{2}$$

where D_0 and D_i are the brushborder tube and core diameters, respectively, L its length, and Q_C the flow rate in the brushborder core devoid of inserts. The last term represents the effect of slip. In its absence, $Q_B = 0$ and Eq. (2) reduces to Poiseuille's law.

We note that Eq. (2) is quite generally valid for viscous flow in tubes with uniform wall protuberances, subject only to the assumption that slip velocity equals the average axial velocity in the wall structure. A more precise evaluation of slip is difficult to make because of the heterogeneous nature of the brushborder/core interface.

To obtain flow ratios in brushborders without inserts from these measurements, Q_B/m, is substituted in Eq. (2), yielding:

$$Q_B/Q_C = \frac{128\, m L (D_o^2 - D_i^2)}{128\, m L D_i^2 + \pi D_i^4 (D_o^2 - D_i^2)} \tag{3}$$

2. Experiments without Tubular Inserts

In the absence of core inserts, the first term on the right side of Eq. (2) equals 1/2 (V_C/t), where V_C is now the volume of the brushborder core, t the transit time of the dye tip through it. Noting that $Q_B = Q_T - Q_C$

Table 2. Measured average ratios of brushborder to core flow

Brush type	Average brush void fraction ε	Brushborder tube diameter D_0 (cm)	Core diameter D_i (cm)	Flow ratio $(Q_B/Q_C)10^2$ Eq. (3)	Eq. (4)
Brushlon	0.839	2.76	0.997	3.2	5.2
Own construction	0.892	3.27	1.119	8.9	–
Pipe cleaners					
High density	0.950	3.29	1.491	7.8	6.7
Medium density	0.975	3.20	1.488	17.1	16.8
Low density	0.987	3.20	1.487	38.5	36.0

and rearranging Eq. (2) one obtains, in terms of the measured variables

$$Q_B/Q_C=\frac{(D_o^2/D_i^2-1)(2Q_T-V_C/t)}{(V_C/t)(D_o^2/D_i^2-1)+2Q_T}. \quad (4)$$

Table 2 shows a comparison of flow ratios calculated from transit times measured both with and without tubular inserts (Eqs. (3) and (4)). The values cited represent an average of some 15 to 45 measurements for each brushborder tube over the range $Re=0.01-0.2$. Agreement between the two sets of results is seen to be satisfactory. The values obtained without inserts, however, are somewhat less reliable because of the difficulty in estimating errors in core geometry and transit time.

Discussion

1. *Correlation and Prediction of Results*

One important result which emerges from this study is that fractional flow through the brushborder, and by extension Q_B/Q_C, is independent of Reynolds number within experimental error. Figure 4 shows this for the set of pipe cleaner brushes fitted with tubular inserts, indicating that the flow regimes in both core and brushborder are essentially identical. Similar results were obtained in the runs without inserts.

In order to interpret these observations and allow them to be extrapolated to other configurations, we considered ways of correlating flowrate with the geometrical parameters of the structure. We drew for this purpose on the Kozeny-Carman equation which gives the relation between superficial velocity U and pressure drop $\Delta P/L$ in assemblies of solid particles of arbitrary shape [2, 5].

$$U=\frac{\Delta P}{L}\frac{\varepsilon^3}{(1-\varepsilon)^2}\frac{1}{\mu k(S/V)^2} \quad (5)$$

where ε, S, V are bed void fraction, particle surface area, and volume, respectively, and k = Kozeny's constant. The expression is based on Poiseuille flow through an array of parallel channels of arbitrary shape and is quite generally valid for laminar flow through beds of particles. Extensions to turbulent flow also exist [2]. In beds of low porosity ($\varepsilon<0.4$), Kozeny's constant is approximately 5. At higher va-

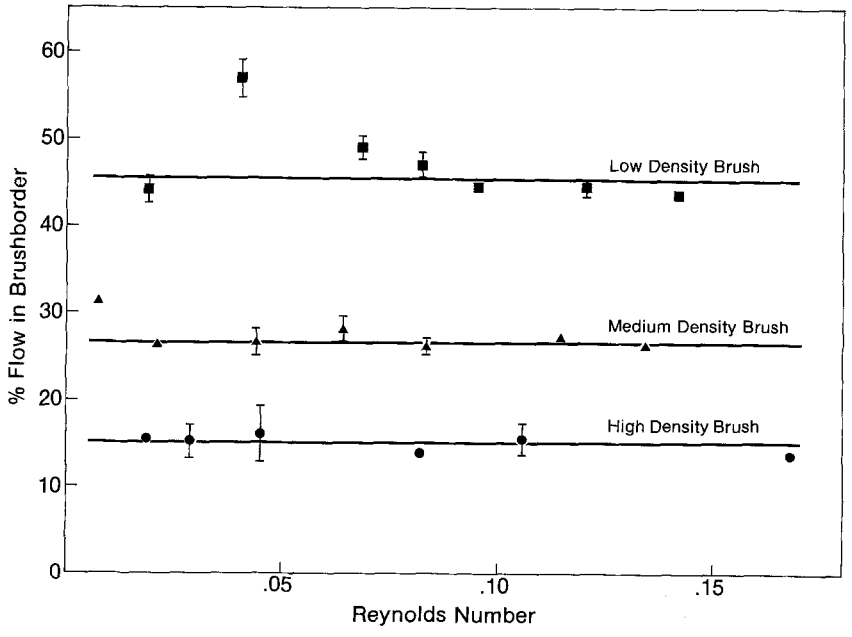

Fig. 4. Plot of % flow in brushborder *vs.* Reynolds number for pipe cleaner brushes with tubular inserts (uncorrected)

lues of ε, k becomes dependent on porosity. For flow perpendicular to an array of parallel cylinders, this dependence is given by [5]:

$$k=\frac{2\varepsilon^3}{(1-\varepsilon)\left[\ln\left\{\frac{1}{1-\varepsilon}\right\}-\left\{\frac{1-(1-\varepsilon)^2}{1+(1-\varepsilon)^2}\right\}\right]}. \tag{6}$$

To obtain an expression for Q_B/Q_C from these relations, we expressed Eq. (5) in terms of flow rate through an annular array of parallel cylindrical bristles:

$$Q_B=\frac{\pi\Delta P}{64\mu L}\frac{\varepsilon^3}{(1-\varepsilon)^2}\frac{D_{Br}^2(D_o{}^2-D_i{}^2)}{k} \tag{7}$$

where D_{Br} is the bristle diameter.

Combining this equation with Poiseuille's law corrected for slip (Eq. (2)), and using the appropriate expressions for Kozenys constant, one obtains

For $\varepsilon>0.4$:

$$\frac{Q_B}{Q_C}=\frac{D_{Br}^2(D_o{}^2-D_i{}^2)\left[\ln\left(\frac{1}{1-\varepsilon}\right)-\frac{1-(1-\varepsilon)^2}{1+(1-\varepsilon)^2}\right]}{(1-\varepsilon)D_i{}^4+D_{Br}^2D_i{}^2\left[\ln\left(\frac{1}{1-\varepsilon}\right)-\frac{1-(1-\varepsilon)^2}{1+(1-\varepsilon)^2}\right]} \tag{8}$$

and for $\varepsilon<0.4$:

$$\frac{Q_B}{Q_C}=\frac{2\varepsilon^3D_{Br}^2(D_o^2-D_i{}^2)}{5D_i{}^4(1-\varepsilon)^2+2\varepsilon^3D_{Br}^2D_i{}^2}. \tag{9}$$

The second term in the denominator of these equations represents the effect of interfacial slip. Similar expressions can be derived for other protuberant shapes, starting with the general Eqs. (2) and (5), or their analogue for the turbulent regime [2] and using tabulated values for Kozeny's constant for void fractions above 0.4 [5]. Flow through open channels or structures such as external growths on animal limbs can also be accommodated by replacing the modified Poiseuille equation (Eq. 2)) with an appropriate relation for flow in or around the support structure.

A double logarithmic plot of Eq. (8) is shown in Fig. 5. ε was calculated by subtracting total bristle volume from total annular space. The values represent an average of the local void fractions which generally drop from a high at the tube wall to a minimum at the bristle tips (*see* Table 1).

The experimental Q_B/Q_C values are seen to give reasonable agreement with the theoretical equation. The largest deviation occurs in the tube containing

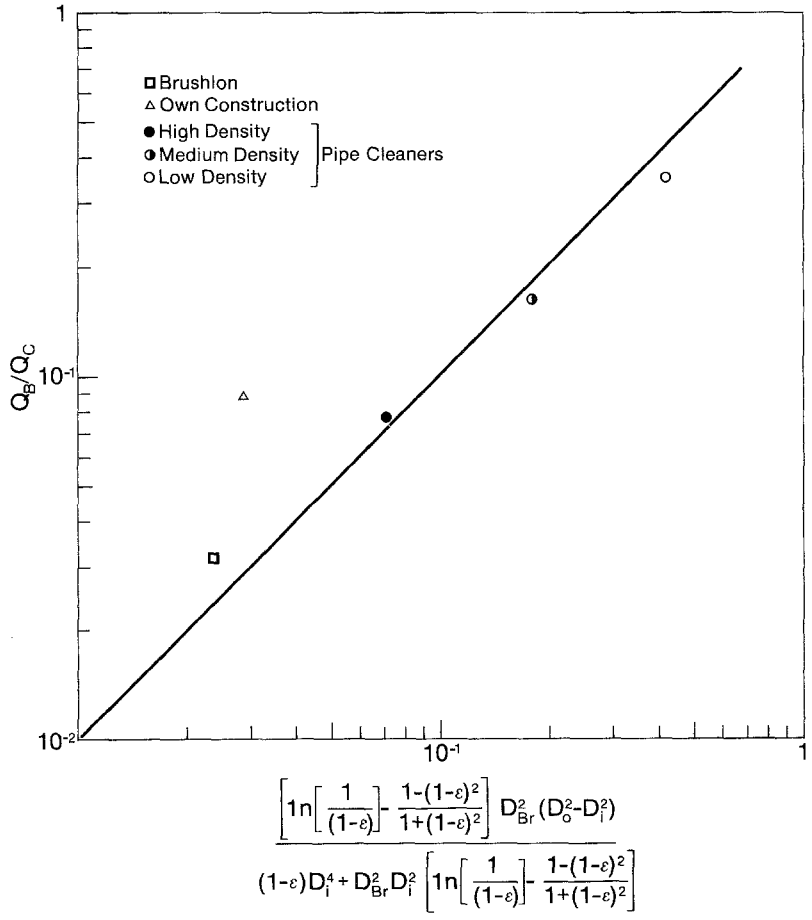

Fig. 5. Experimental ratios of brushborder to core flow, compared with the predictions of Eq. (8) (—)

bristles mounted in tufts, i.e., the configuration which differs most significantly from the assumed model of parallel cylinders. The Brushlon tube also shows some deviation from the predicted value, probably due to a slight assymmetry in the tube construction.

2. *Flow Through Proximal Tubular Brushborders*

Before applying these findings to flow in the proximal tubule and similar structures, consideration had to be given to the effect of radial flux on brushborder flow. Marshall and Trowbridge [6] have shown that for flow in smooth cylindrical tubules with leakage, a correction factor Γ must be applied to Poiseuille's law, which is now written in differential form to allow for varying flow rates:

$$\frac{dP}{dz} = -\Gamma \frac{128\,\mu}{\pi D_i^4} Q. \tag{10}$$

Γ ($\leqq 1$) was found to depend only on wall permeability K, wall thickness t, and on lumen radius a; it was not affected by axial velocity. Furthermore, for conditions prevailing in the proximal convoluted tubule, the correction factor reduces to the simple expression [6]:

$$\Gamma = 1 - \frac{16}{3}\frac{K}{ta}. \tag{11}$$

Calculated values for K/ta in *PCT* were in the range $10^{-6}-10^{-8}$ [6] so that $\Gamma \approx 1$ and Poiseuille's law remains valid in its differential form.

To apply these findings to flow in the brushborder, we recall that the Kozeny-Carman equation is based on the concept of Poiseuille flow through a bundle of parallel tubes, appropriately corrected for deviations from straight cylindrical form. If we consider the extreme example of a *single* axial pore in the brushborder subjected to the same fractional reabsorption as the *PCT*, and set its radius at 0.01 a (roughly equivalent to the bristle radius), Kt/a increases at most to 10^{-4} so that the correction to Poiseuille flow is still negligible. This implies that the differential form of the Kozeny-Carman equation (Eq. (7)) is a valid representation of brushborder flow in the presence of transtubular flux of the magnitude encountered in *PCT*. Division of the differential Kozeny-Carman and Poiseuille equations leads to the same expressions for fractional flow (Eqs. (8) and (9)) we used previously to interpret our model experiments.

We therefore felt able to use these equations to obtain an estimate of fractional flow rates in the proximal tubule. The physical parameters were calculated from data provided by Welling and Welling [10] on rabbit proximal tubular brushborders. In the proximal convoluted tubule, depending upon the analytical method used, they found 11.6 to 41.0 microvilli/μm^2 of apical cell surface, the latter being the preferred density. Under the conditions of their study, the diameter of the tubule to the base of the brushborder was 25.3 μm; the microvilli were at least 2.8 μm long and 0.1 μm in diameter [9]. These figures were used to obtain the volume of microvilli/μm length of proximal convoluted tubule.

Table 3 shows the results of our calculations for a proximal tubule in various states of dilation. Void fractions ε_1 and ε_2 correspond to the two densities of 11.6 and 41.0 microvilli/μm^2 and were calculated by assuming that the volume and length of the microvilli remain constant as the proximal tubule dilates and collapses. With these values, flow through the denser brushborder is found to be vanishingly small, while the sparser growths give flows of the order 0.01–0.1%. These results are surprisingly low considering the substantial fraction of free area residing in the brushborder (Table 3) and reflect the high frictional resistance to axial flow in these structures.

It is of some interest to consider the possible effect of these flow rates on radial solute distributions in the proximal tubule. Recent theoretical studies by Passow [7] and Richardson et al. [8] have indicated that significant radial concentration gradients could arise in brushborders and folded membranes. These studies assumed an absence of longitudinal transport, but Richardson et al. demonstrated that partial "stirring" between folded membranes would alter relative

Table 3. Calculated ratio of brushborder to core flow in proximal tubules of various diameters

Tubule diameter D_0 (μm)	Core diameter D_i (μm)	Brushborder Void fraction		Brushborder void volume / Central luminal volume (for ε_2)	Flow Ratio $(Q_B/Q_C)10^2$	
		Low density (ε_1)	High density (ε_2)		For ε_1	For ε_2
25.6	20	0.90	0.64	0.41	0.02	0.001
20.6	15	0.87	0.54	0.49	0.03	0.001
15.6	10	0.82	0.36	0.53	0.06	0.0007
13.6	8	0.79	0.24	0.46	0.09	0.0003

solute to water flux. Such stirring might conceivably be brought about by either longitudinal transport in the brushborder, or by motions of the microvilli themselves.

The flow ratios we calculated for proximal tubules (Table 3) translate into local brushborder velocities of $4\times10^{-4}-4\times10^{-5}$ cm/sec for the sparse structure, and 3 to 4×10^{-6} cm/sec for the denser growth. These figures are based on a total flowrate of 20 nl/min in the tubule and are sufficiently low for molecular diffusion to be a significant or even preponderant component of axial transport. Assuming a linear solute gradient in a tubule 0.5 cm long, solute diffusivity of 2×10^{-5} cm^2/sec translates roughly into an axial diffusive velocity of the order 4×10^{-5} cm/sec. This means that longitudinal transport in the sparse brush would be both convective and diffusive, while the denser – and preferred – configuration would have preponderantly diffusive transport which is *flow insensitive* at the low axial flows in question. It does not seem likely, therefore, that axial transport in the brushborder would bring about either a partial stirring of brushborder fluid or provide a mechanism for flow-sensitive reabsorption as envisaged by Giebisch [4] and Richardson et al. [8]. Motions of the microvilli themselves are also unlikely to provide the necessary turbulence: Assuming that they move at a frequency of 1–10 times every second over a rather exaggerated distance of 1 μm, their motion would be equivalent to a convective velocity of only 10^{-4} to 10^{-3} cm/sec. It appears from these figures that the brushborder fluid in the proximal tubule is unlikely to be stirred to any significant degree, even if the microvilli are mobile as DeWardener [3] and others have postulated.

Conclusions

Fractional axial flow through synthetic brushborder tubes has been found to be independent of Reynolds number in the range 0.01–0.2. The data can be correlated by means of theoretical equations based on the Kozeny-Carman relation for flow through arrays of solid particles. Extension of the correlation to higher Reynolds numbers and other geometries can be achieved by simple modifications in the basic flow equations. The results indicate that axial transport in the brushborder of the proximal tubule will be predominantly diffusive in nature, and that neither luminal flow velocity nor movement of microvilli are likely to significantly alter radial solute gradients in the brushborder.

We wish to thank R. Chachel and J. Furman, who contributed to the initial stages of the work and the 3M Corporation for providing samples of their Brushlon product. The support received from a Medical Research Council of Canada Grant (MRA 3045) is gratefully acknowledged.

References

1. Baker, D.J. 1968. A technique for the precise measurement of small fluid velocities. *J. Fluid Mech.* **26** (3):573–575
2. Bird, R.B., Stewart, W.E., Lightfood, E.N. 1960. Transport Phenomena. p. 200. John Wiley & Sons, New York
3. De Wardener, H.E. 1978. The control of sodium excretion. *Am. J. Physiol.* **235**:*F*163–*F*173
4. Giebisch, E. 1978. The proximal nephron. *In*: Physiology of Membrane Disorders. T.E. Andreoli, J.F. Hoffman, and D.D. Fanestil, editors. p. 697, Plenum Medical
5. Happel, J., Brenner, H. 1965. Low Reynolds Number Hydrodynamics. pp. 392–399. Prentice-Hall, Englewood Cliffs
6. Marshall, E.A., Trowbridge, E.A. 1974. Flow of a Newtonian fluid through a permeable tube. The application to the proximal renal tubule. *Bull. Math. Biol.* **36**:457–475
7. Passow, H. 1967. Steady-stage diffusion of non-electrolytes through epithelial brushborders. *J. Theoret. Biol.* **17**:383–398
8. Richardson, I.W., Likko, V., Bartoli, E. 1973. The nature of passive flows through tightly folded membranes. The influence of microstructure. *J. Membrane Biol.* **11**:293–308
9. Rostgaard, J., Thuneberg, L. 1972. Electron microscopical observations of the brushborder on proximal tubular cells of mammalian kidney. *Zeit. Zellforsch.* **132**:473–496
10. Welling, L.W., Welling, D.J. 1975. Surface areas of brushborder and lateral cell walls in the rabbit proximal nephron. *Kidney Int.* **8**:343–348

Received 9 October 1979; revised 25 March 1980